Experimental Thermal and Fluid Science 56 (2014) 23–32

Contents lists available at ScienceDirect

Experimental Thermal and Fluid Science

journal homepage: www.elsevier.com/locate/etfs

Flame structure of methane inverse diffusion flame

A.M. Elbaz [a,b,*], W.L. Roberts [a]

[a] Clean Combustion Research Center, King Abdullah University of Science and Technology (KAUST), Jeddah 23955-6900, Saudi Arabia
[b] Mechanical Power Engineering Department, Faculty of Engineering, Helwan University, Cairo 11718, Egypt

ARTICLE INFO

Article history:
Available online 28 November 2013

Keywords:
Inverse diffusion flames
PLIF-OH imaging
PIV measurements

ABSTRACT

This paper presents high speed images of OH-PLIF at 10 kHz simultaneously with 2D PIV (particle image velocimetry) measurements collected along the entire length of an inverse diffusion flame with circumferentially arranged methane fuel jets. For a fixed fuel flow rate, the central air jet Re was varied, leading to four air to fuel velocity ratios, namely Vr = 20.7, 29, 37.4 and 49.8. A double flame structure could be observed composed of a lower fuel entrainment region and an upper mixing and intense combustion region. The entrainment region was enveloped by an early OH layer, and then merged through a very thin OH neck to an annular OH layer located at the shear layer of the air jet. The two branches of this annular OH layer broaden as they moved downstream and eventfully merged together. Three types of events were observed common to all flames: breaks, closures and growing kernels. In upstream regions of the flames, the breaks were counterbalanced by flame closures. These breaks in OH signal were found to occur at locations where locally high velocity flows were impinging on the flame. As the Vr increased to 37.4, the OH layers became discontinuous over the downstream region of the flame, and these regions of low or no OH moved upstream. With further increases in Vr, these OH pockets act as flame kernels, growing as they moved downstream, and became the main mechanism for flame re-ignition. Along the flame length, the direction of the two dimensional principle compressive strain rate axis exhibited a preferred orientation of approximately 45° with respect to the flow direction. Moreover, the OH zones were associated with elongated regions of high vorticity.

1. Introduction

Non-premixed flames are employed in the majority of practical combustion systems, principally due to the ease with which these flames can be controlled [1]. Inverse jet diffusion flames (IDF), in which a central oxidizer is injected into an abundance of co-flowing fuel have been studied for many years [2,3]. Characteristics and structure of nominally non-premixed flames of natural gas were investigated by Sobiesiak and Wenzell [2], using a burner that employs two distinct features: fuel and oxidizer direct injection, and inverse fuel and oxidizer delivery. The mean temperature, and temperature fluctuations profiles, together with Schlieren images, indicate the presence of partial premixing in this non-premixed IDF configuration of reactants. The region of partial premixing subsequently evolves into a well-mixed reaction zone on the flame centerline enveloped by an outer diffusion flame. They also concluded that the degree of partial premixing on the flame centerline depends on the nozzle geometry and the flow conditions. The radiation emission from diffusion flames is very dependent on the manner in which the combustion is carried out; where the most striking difference between the normal diffusion flame and the IDF flames is the much stronger luminosity and soot radiation of the normal flame [3].

Wu and Essenhigh [4] reported experimental and predicted temperature and composition profiles of stable species at different axial locations in laminar methane IDF flames. Six different flames types were identified in their mapping of IDF methane flame. They identified two similar types to be the most "representative" of the IDFs; they covered more than 50% of the total flame map. The structure of this flame has a parabolic main blue combustion zone. A yellow zone starts about 1/3 of the way up the side of the blue zone and is something of a tapered, truncated annulus, open at the top and thus enclosing a dark zone above the top of the blue zone.

The multi-inverse diffusion flame is a special case of the traditional IDF, where the outer annular fuel jet is subdivided into multiple circumferential fuel jets surrounding the inner air jet. The central air jet entrains the fuel jets toward the air jet, consequently, better flame stability and good mixing between the fuel and air jets can be achieved [5]. The multi fuel jet inverse diffusion flame compared to the traditional IDF was able to operate stably even with very low Re number [5]. In lieu of any direct knowledge of the

* Corresponding author. at: Address: Clean Combustion Research Center, King Abdullah University of Science and Technology (KAUST), Jeddah 23955-6900, Saudi Arabia. Tel.: +966 0128084645.

E-mail address: ayman.elhagrasy@Kaust.edu.sa (A.M. Elbaz).

0894-1777/$ - see front matter © 2013 Elsevier Inc. All rights reserved.
http://dx.doi.org/10.1016/j.expthermflusci.2013.11.011

velocity field in IDFs, some authors have presumed that the velocity field is similar to that of a normal diffusion flame (NDF), wherein co-flow (air) entrainment dominates near the base of the flame, giving a radial inflow, followed by more or less vertical, buoyancy dominated flow [6].

It is clear then that most of the work concerning the IDFs have focused on flame appearance, temperature profile and emissions. This work uses high speed OH-PLIF collected at 10 kHz simultaneously with 2D PIV measurements in a methane inverse diffusion flame with multiple fuel jets, to better understand the role of mixing and entrainment in these flames, spatial flame structure. With a constant fueling rate, the effect of the air flow rate, in terms of air Reynolds number which leads to four flames of different air/fuel velocity ratios (Vr = Va/Vf), was investigated.

2. Experimental set up and methodology

The burner geometry used in this study is shown in Fig. 1(a). It consists of an inner air jet of 4.3 mm in diameter, surrounded by an annular 0.81 mm fuel slit, with a center–center distance of 9 mm between the air and fuel annular jets. This annular separating distance between the annular fuel jet and central air jet creates a bluff body to improve the flame stability. To reduce the air entrainment to the flame from the surroundings and to decrease flame instabilities caused by room air currents, the burner was confined by a 40 × 30 × 80 cm^3 Pyrex shield with small openings to admit lasers light. The distance between the centers of the burner to the wall of the shield is relatively two high. This is to eliminate the boundary layer effect of the rectangular shield on the axis-symmetrical circular flame burner. A uniform fuel distribution at the burner exit could be achieved, where the distance between the fuel entrances of the burner to the fuel jet exit is relatively long. it is The experiments were carried out with a fixed fueling rate while the air jet Re was varied from 2500 to 6000, leading to four velocity ratios in the range of 20.7–49.8. The details of the flow conditions are given in Table 1. In IDFs the fuel and air jets are issuing separately and the concept of equivalence ratio may not be directly applicable to the IDFs, however it has been indicted in Table 1, and this is to give an indication of the relative strength of the air and fuel supply compared to the stoichiometric air/fuel ratio. The experimental configuration is illustrated in Fig. 1(b). The system consists of 2D PIV set up and OH-PLIF imaging system with overlapping fields of view. The system was used to acquire 2D velocity measurements in a plane and simultaneously track the spatial and temporal features of the OH-LIF images at 10 kHz repetition rate.

A schematic of the high-speed OH-PLIF imaging set up is shown in Fig. 1(b). Laser light was used to excite the Q1(6) line of the $A^{2\text{-}}\sum \leftarrow X^{2\Pi}$ (1,0) system at 283.01 nm. The OH-PLIF system used a frequency-doubled high speed dye laser (Sirah, Cerdo-Dye) pumped with a frequency-doubled, diode-pumped solid state laser (Edgewave IS16II-E). Using Rhodamine 6G, the dye laser produced a fundamental beam at 566 nm, which was then frequency doubled using a BBO crystal to produce a UV beam at 283 nm. The OH fluorescence signal was acquired with a High-Speed-Star 8 CMOS camera (LA Vision HSS8) and an external two-stage, lens-coupled intensifier (La Vision HS-IRO) with a 100 mm, f/2.8 UV-objective (LA Vision. GmbH). The camera has 1024 × 1024 pixels imaging array at a repetition rate of 7.5 kHz. Elastic scattering at 283 nm was blocked using a transmission (>80% at 310 nm) band-pass interference filter (Custom Fabrication-Laser-Components GmbH). Each OH-PLIF image is corrected for background and for shot–shot laser fluctuations. The sheet profile correction was determined via an ensemble average of 10,000 individual images of the laser sheet passing through a couvette filled with acetone placed in the center of the field of view.

The two dimensional PIV system consisted of a dual cavity, diode-pumped, solid state Nd: YLF laser (LDY 300 Series) and a single CMOS camera (La Vision, image pro HS 4M), with 9 ns pulse duration. Pulses were formed into a sheet with a 0.5 mm waist along the jet centerline using three cylindrical lenses. Both the air and fuels jets were seeded with titanium dioxide (TiO_2) particles with a nominal diameter of 0.5 μm via particle plaster seeding unit. Mie scattered light from the particle laden flow was collected using 105 mm, f/4 objectives (Nikon UV Micro-Nikkor) equipped with 527 nm band pass interfacing filters. The camera was operated in two-frame burst mode at 500 fps. Vector fields were computed from particle image spatial cross correlation using the La Vision Davis 8.1 software package. An adaptive multi-pass vector evaluation technique was used, with interrogation boxes ranging from 128 pixels to 32 pixels, resulting in a spatial resolution and vector spacing of approximately 0.5 mm and 0.25 mm, respectively.

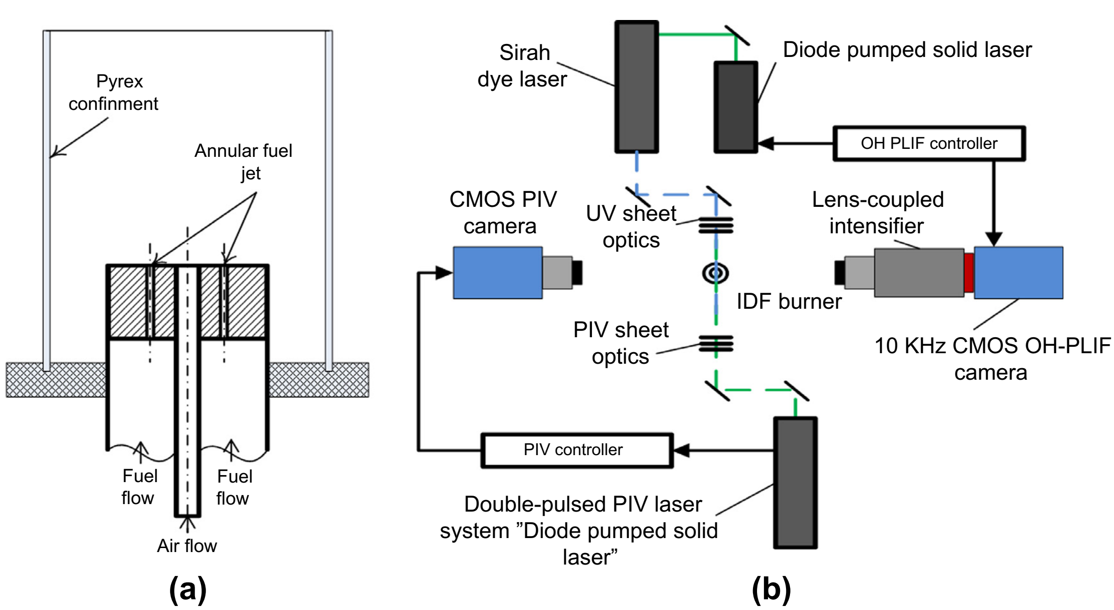

Fig. 1. IDF burner (a) and experimental set up (b).